Simultaneous surface display and cargo loading of encapsulin nanocompartments and their use for rational vaccine design

Priscillia Lagoutte [a], Charlotte Mignon [a], Gustavo Stadthagen [a], Supanee Potisopon [a], Stéphanie Donnat [a], Jan Mast [b], Adrien Lugari [a,*], Bettina Werle [a,*]

[a] BIOASTER, Protein and Expression System Engineering unit, 40 avenue Tony Garnier, 69007 Lyon, France
[b] Service Trace Elements and Nanomaterias, Sciensano, Groeselenbergstraat 99, B-1180 Brussels, Belgium

ARTICLE INFO

ABSTRACT

In the past decades protein nanoparticles have successfully been used for vaccine applications. Their particulate nature and dense repetitive subunit organization makes them perfect carriers for antigen surface display and confers high immunogenicity. Nanoparticles have emerged as excellent candidates for vectorization of biological and immunostimulating molecules. Nanoparticles and biomolecular nanostructures such as ferritins or virus like particles have been used as diagnostic and therapeutic delivery systems, in vaccine development, as nanoreactors, etc. Recently, a new class of bacterial protein compartment has been discovered referred to as encapsulin nanocompartment. These compartments have been used for targeted diagnostics, as therapeutic delivery systems and as nanoreactors. Their biological origin makes them conveniently biocompatible and allows genetic functionalization. The aim of our study was to implement encapsulin nanocompartements for simultaneous epitope surface display and heterologous protein loading for rational vaccine design. For this proof-of-concept-study, we produced *Thermotoga maritima* encapsulin nanoparticles in *E. coli*. We demonstrated the ability of simultaneous display in our system by inserting Matrix protein 2 ectodomain (M2e) of influenza A virus at the nanoparticle surface and by packaging of a fluorescent reporter protein (GFP) into the internal cavity. Characterization of the nanoparticles by electronic microscopy confirmed homogenously shaped particles of 24 nm diameter in average. The results further show that engineering of the particle surface improved the loading capacity of the heterologous reporter protein suggesting that surface display may induce a critical elastic deformation resulting in improved stiffness. In Balb/c mice, nanoparticle immunization elicited antibody responses against both the surface epitope and the loaded cargo protein. These results confirm the potential of encapsulin nanocompartments for customized vaccine design and antigen delivery.

© 2018 Elsevier Ltd. All rights reserved.

1. Introduction

For several decades, nanoparticles, and in particular Virus like Particles (VLPs) based on subunits of viral surface proteins have been commercialized as vaccines in human health against human hepatitis B virus, hepatitis E virus and Human Papilloma Virus [1], and in animal health against porcine circovirus type II [2].

These vaccine delivery systems attempt to mimic various properties of pathogens and thereby increase immunogenicity.

Diverse delivery systems are currently under development. Examples include nanoparticles which have dimensions that are similar to those of microbial pathogens. Such particulate delivery systems constitute a heterogeneous category of carriers including protein cage based [3–6], liposomes [7,8] and inorganic and polymeric nanoparticles [9–11]. In contrast to lipid based, polymer-based or inorganic-based, protein based nanoparticles are biocompatible systems composed of multiple copies of one or few subunits leading to repetitive structures that auto-assemble having highly uniform size and symmetry [12,13]. This particulate nature and high repetitive surfaces makes them ideal carriers for antigen and epitope surface display (unrelated to the nanoparticles itself) and confers high immunogenicity [13]. The most frequently used

nanoparticles carriers are derived from viral coat proteins, in particular from bacteriophages (MS2, Qβ, P22), from hepatitis B virus (core and surface protein) or from plant viruses (Cowpea chlorotic mottle virus and Cowpea mosaic virus) [14]. Antigens and epitopes are displayed on the surface by genetic fusion or by conjugation systems [3,13–21]. Besides surface display nanoparticles have emerged as excellent candidates for vectorization systems of biological molecules as nucleic acid, CpGs, proteins or other immunostimulation molecules [13,14,22,23].

In the present study we engineered recently discovered virus capsid-like nanocompartments called encapsulin as nanocarrier particle for customized epitope display and cargo protein vectorization. Encapsulin nanocompartments have been discovered in different bacteria and archaea including medically important species such as *Mycobacterium tuberculosis* [24–27]. Even if their biological functions are not completely elucidated, McHugh et al., [28] have recently shown that these nanocompartments could store iron and protect bacteria from oxidative stress. *Thermotoga maritima* [24], *Mycobacterium tuberculosis* [29] and *Rhodococcus erytropolis/josti* [30] nanocompartments consist of 60 copies of identical subunits that form a T = 1 icosohedral capsid-like particles of 20–24 nm. In contrast, *Pyrococcus furiosus* [25] and *Myxococcus xanthus* [28] nanocompartments contain 180 protein subunits that form a T = 3 icosahedral particle with a diameter of 30 to 32 nm. In bacteria, encapsulin compartments have the ability to package functional enzymes such as ferritin-like proteins and Dyp-type peroxidases [24,28,29]. These encapsulated proteins have a specific C-terminus sequence that leads them to bind to the interior surface of encapsulin [24]. This specific cargo-loading capacity has been used to package non-native cargo proteins [31,32]. Various applications of encapsulin-based nanocompartments have been nicely reviewed by T. Giessen [6]. Among these, Moon et al., demonstrated the use of the engineered encapsulins from the thermophilic *T. maritima* for targeted diagnostics and targeted therapeutic delivery [33]. More recently, specific loading of heterologous cargo proteins as eGFP and luciferase inside the encapsulin compartment from *R. erythropolis* N771 and *Brevibacterium linens* has been described. However the packaging efficacy of both guest proteins was either low [31,32,34], or loading destabilized the correct assembly of the nanocompartment [35].

In the present study we describe the engineering of thermophilic encapsulin *T. maritima* to generate a multifunctional nanoplatform for simultaneous heterologous protein loading and epitope surface display. We engineered *T. maritima* eGFP loaded encapsulin nanoparticles that display the Matrix protein 2 ectodomain epitope of the influenza A virus [36] at their surface. After purification, the potential of the packaging efficiency was demonstrated. Immunogenicity studies revealed antibody responses against both the surface epitope and the loaded cargo protein after immunization of Balb/c mice. These new findings confirm the potential of encapsulin nanocompartments as a versatile nanoparticle carrier for rational vaccine design and antigen delivery [6,37].

2. Materials and methods

2.1. Construction of the plasmids

Four encapsulin constructs (NC000853; GI:1564277) carrying the previously described C200S mutation [33] were generated as shown in Fig. 1. The first construct (NP) encodes the encapsulin gene under the control of the T7 promoter. The second and third constructs contain bicistronic cassettes encoding both: eGFP fused to the C-terminal extension sequence of the ferritin-like protein (IEEETSGGSENTGGDLGIRKL; GI:15642775) annotated as flp tag and the encapsulin gene without (NPGFP) and with an insertion of the M2e epitope GGEVETPIRNEGG from *Influenza A* virus H1N1 (GI:21693176) between amino acid positions 138 and 139 (NP$_{M2e}$-GFP). The fourth construct is identical to NPGFP with an additional Hexahistidine peptide (NP$_{His}$GFP) inserted between amino acid positions 42 and 43 which was previously described to improve particles heat stability [33]. As a positive control of M2e display,
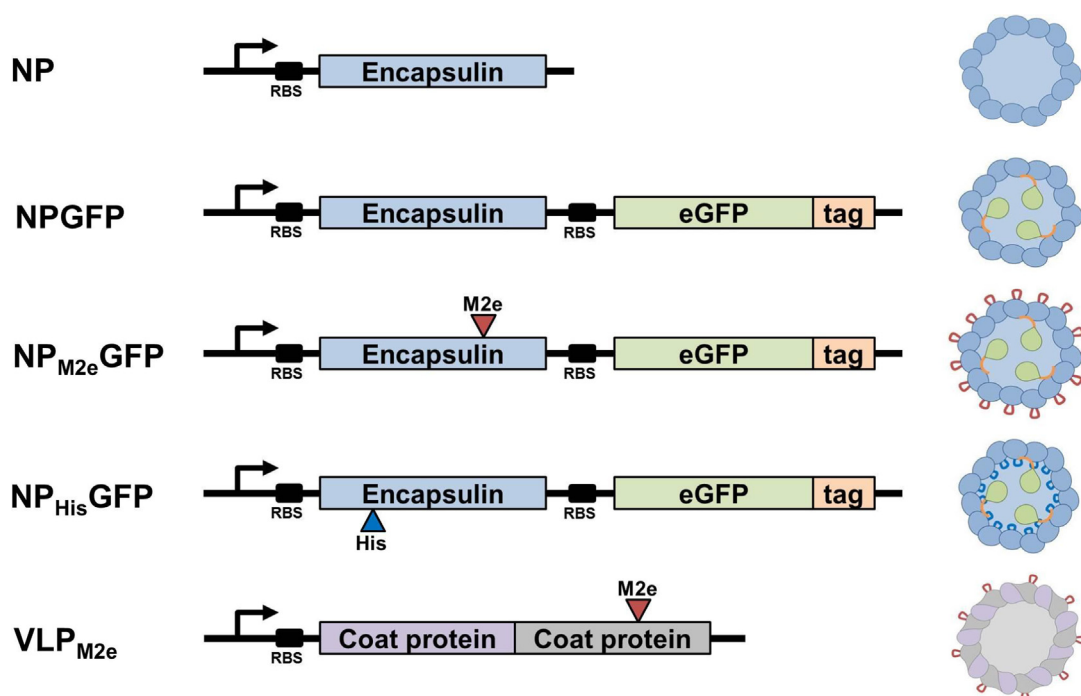

Fig. 1. Schematic representation of genetic constructs designed for nanoparticle generation. Color code : encapsulin in light blue; eGFP in green; flp tag in orange; M2e (ectodomain of Matrix protein) in red; HexaHis (HexaHistidine peptide) in dark blue; coat protein dimer (MS2 bacteriophage) in purple and grey respectively; RBS (ribosome binding protein) in black. (For interpretation of the references to color in this figure legend, the reader is referred to the web version of this article.)

we generated bacteriophage MS2 based VLPs presenting M2e epitope (VLP$_{M2e}$) as previously described in detail [38].

According to the crystallographic structure of encapsulin [24], M2e epitope inserted between amino acid positions 138 and 139 is exposed on the particle surface whereas HexaHistidine peptide insertion between amino acid positions 42 and 43 leads to internal peptide presentation.

2.2. Expression and purification of encapsulin mediated nanoparticles

Plasmids were transformed into competent Escherichia coli BL21(DE3). One liter batch was grown in LB medium supplemented with 50 μg mL^{-1} Kanamycin (Sigma Life Science) for 3 h at 37 °C, shaking at 180 rpm. Protein expression was induced with 100 μM IPTG at 18 °C overnight, with shaking at 180 rpm. Cells were harvested by centrifugation at 10000g (5 min). Cells pellets were resuspended in 25 mL of phosphate buffer saline (137 mM NaCl; 2.7 mM KCl; 10 mM Na$_2$HPO$_4$; 1.76 mM KH$_2$PO$_4$) and 0.1 mg ml^{-1} DNase. Cell lysis was carried out by mechanical disruption using silica beads (Matrix B) and a FastPrep device (MPbio) prior to centrifugation (17000g) for 20 min. The resulting supernatant was filtered (0.22 μm) in order to remove cells debris. Nanoparticles were then purified as described previously [38].

2.3. Protein quantification

The protein concentration was determined using BCA method with bovine serum albumin as standard. Protein was analyzed by SDS-PAGE 4–12% (Biorad) and stained with Imperial protein stain (Thermo). Western-blot experiments were performed using mouse monoclonal antibodies against GFP and epitope M2e. A secondary goat anti-mouse antibody coupled to fluorophore Alexa 647 was used for the blot revelation.

2.4. Analysis by transmission electron microscopy (TEM)

Samples were negatively stained and nanoparticles size, morphology and concentration were determined by TEM as previously described [39]. Briefly, samples were negatively stained on grids pre-treated with Alcian blue. Grids were deposited on a 15 μL drop of nanoparticles containing solution for 10 min and rinsed two times with water. Afterwards, the grids were stained for 10 s on a drop of 2% uranyl acetate (Agar Scientific), blotted and airdried. The samples were imaged in bright field (BF) mode using a Tecnai Spirit TEM (FEI) with Biotwin lens configuration operating at 120 kV. Micrographs were recorded using a 4 × 4 K CCD camera (Eagle, FEI) at a magnification of 30,000 times. The estimation of the number of particles per ml is based on the correlation between the amount of particles in suspension and the number of particles attached to a specific area of the EM-grid. The latter is estimated by counting the number of particles in representative transmission electron micrographs (n ≥ 20).

2.5. Packaging performance assay

The number of packaged protein molecules was estimated by measuring the relative intensity of fluorescence (CFX96 TouchTM Real-Time PCR Detection System, Bio-Rad). Briefly, a standard curve of purified eGFP (from 0 to 30 μg mL^{-1}) was generated and fluorescence emission spectra measured at 504 nm using a spectrophotometer. For each of the nanoparticles samples NP, NPGFP, NPM2eGFP and NPHisGFP, the fluorescence intensity was measured. In parallel, the protein concentration was determined using a NanoDrop (Spectrophotometer) at OD280nm. Once the encapsulin and eGFP concentrations have been determined, their ratio represents an estimate of the number of eGFP loaded molecules.

Table 1
Estimation of loading capacity per nanoparticle.

Construction	Particles/mL	Estimated eGFP per nanoparticle
NP	4×10^{11}	–
NPGFP	1×10^{8}	0.2 ± 0.18
NP$_{M2e}$GFP	2×10^{11}	32 ± 8.5
NP$_{His}$GFP	1×10^{12}	0.7 ± 0.1

Each experiment is done in triplicate (Table 1). The measurement of eGFP per nanoparticle was adapted from Tamura et al., [32].

2.6. Immunization

Animal experiments were conducted at Charles River (Arbresle, France). Five week old female Balb/c mice (7 animals per group) were immunized 3 times subcutaneously. 50 μg of each antigen (NPM2eGFP, VLPM2e, eGFP) were administrated with Freund's adjuvant at days 0, 14 and 28. One group of 7 mice was administered PBS and Freund's adjuvant as control. Serum samples were collected individually from each mouse at day 0, 14, 28 and 42 and stored at −80 °C.

2.7. Immune response

The dosage of specific antibodies in the serum samples was performed as follows: 96-well microplates were coated overnight at 4 °C with either M2e peptide coupled to streptavidin or eGFP (200 ng). Plates were blocked with 1% BSA and serial ten-fold dilutions of sera (1:100 in 1% BSA-PBS) were added to the wells. After incubation for 90 min at room temperature, antibodies were detected by HRP-conjugated goat anti-mouse IgG (Merck, AP127P). After washing TMB Elisa substrate was added, and the reaction stopped using 2 M H$_2$SO$_4$. The optical density (OD) was measured at 450 nm (OD450). End-point titers were determined as the reciprocal of the highest dilution providing an optical density (OD) twice that of PBS-immune serum.

3. Results

3.1. Encapsulin nanoparticles NP$_{M2e}$GFP are efficiently produced in E coli and co-purified with cargo GFP

To study the genetic engineering of encapsulin nanoparticles as a potential delivery nanoparticle platform, four constructs were generated (Fig. 1). We studied the effect of an additional external surface epitopes (M2e) on heterologous protein packaging and stabilization of the nanoparticle assembly. Furthermore we wanted to confirm the role of internal HexaHistidine peptide on nanoparticle stabilization as described previously [33] and further study its impact on GFP packaging. As a positive control we generated bacteriophage MS2 based VLPs presenting M2e epitope (VLP$_{M2e}$) [38].

The resulting nanoparticles were produced in E. coli and purified as described previously [38] with a three step purification protocol depicted in Fig. 2A. In Fig. 2B, follow up of the purification steps of NP$_{M2e}$GFP reveals after gel filtration (lane 6) that encapsulin and GFP are co-purified and migrate as expected at 31.7 and 29 kDa respectively. The chromatogram of this sample presented in Fig. 2C indicates a double peak representing co-purified encapsulin and GFP.

In Fig. 3 is shown the biochemical characterization of purified nanoparticles analyzed by denaturing SDS-PAGE(A), and after Western blotting using anti-M2e (B) and anti-GFP (C) antibodies. These results show that all particles are purified with high degree of purity. Purified GFP used as control migrates at 28 kDa (A) and is
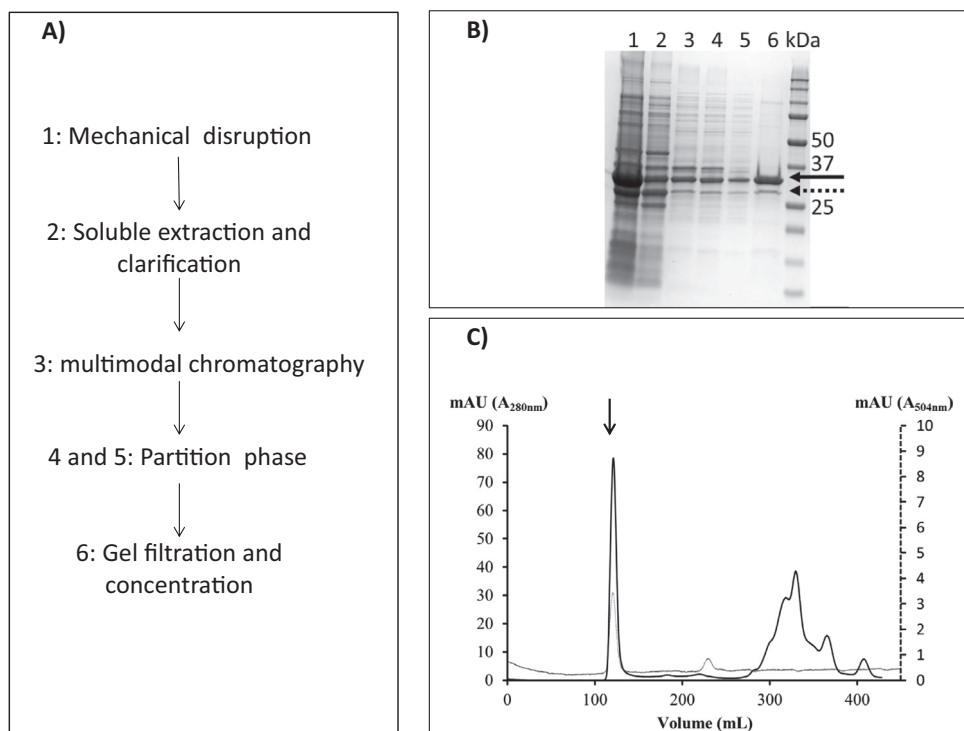
Fig. 2. Purification of encapsulin mediated nanoparticles. (A) Schematic steps of nanoparticles purification and (B) analysis by SDS-PAGE. Lane 1: Bacterial lysate; Lane 2: Soluble fraction filtered; Lane 3: Fraction after multimodal chromatography; Lane 4: Aqueous phase of first separation phase; Lane 5: Aqueous phase of last separation phase; Lane 6: Concentrated fraction after gel filtration. The dotted arrow indicates eGFP and the black arrow indicates encapsulin. (C) Chromatogram of the last step of purification. The grey arrow on chromatogram indicates the double peak consisting of encapsulin and GFP.
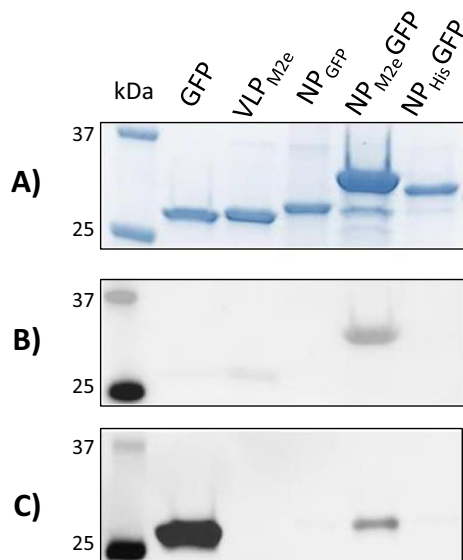

Fig. 3. Biochemical characterization of nanoparticles by SDS-PAGE (A), after Western blotting using anti-M2e (B) and anti-GFP (C) antibodies.

revealed by Western blot using antibody against GFP (C). VLP$_{M2E}$ migrates at 28 kDa (A) and M2e epitope presence is confirmed using anti-M2e antibody (B). NP$_{M2e}$GFP shows correct migration of encapsulin (31.7 kDa) and cargo GFP (29 kDa). Western blot analysis confirms both presence of M2e epitope within the encapsulin protein (B) and cargo GFP (C). Both constructs NPGFP and NP$_{HIS}$GFP show expected encapsulin migration of 31 and 31.9 kDa while cargo GFP loading could not be visualized neither by Coomassie (A) nor by Western blot using anti-GFP antibody (C) suggesting a lack of loading efficiency for both constructs.

3.2. Structural characterization of engineered nanoparticles

To validate correct assembly, purified samples were analyzed by transmission electron microscopy (TEM) as shown in Fig. 4. As expected, wild-type encapsulin (NP) was observed to auto-assemble in icosahedral nanoparticles with a diameter of 24 nm (n = 20). Isolated particles, particles in small agglomerates (2–10 particles) and larger agglomerates were also observed. The larger agglomerates primarily contained wrongly assembled particles of irregular size and morphology. The estimated particle concentration was of 4×10^{11} particles per mL. Coexpression of GFP-cargo and encapsulin (NPGFP) resulted in 1000 × fold fewer nanoparticles (1×10^8 particles per mL) of the expected microstructure of 24 nm diameter. Most of the sample contained wrongly and incompletely assembled nanoparticles and relatively large agglomerates of proteinaceous material. This observation suggests that cargo loading has a destabilizing effect on encapsulin assembly as described previously [35]. Insertion of internal HexaHistidine peptide in encapsulin monomers (NP$_{His}$GFP) resulted in a major population of icosahedral pseudoparticles with a mean diameter of 24 nm (about 1×10^{12} particles per mL). A minor fraction of smaller particles (approximately 10 nm diameter) was also observed. Encapsulin containing the external M2e epitope (NP$_{M2e}$-GFP) auto-assembled in nanoparticles of icosahedral shape and expected 24 nm diameter within a major population estimated at 2×10^{11} particles per mL. Most of the particles were isolated, although some small agglomerates of 10 to 50 particles were also observed.

These results indicate that packaging of heterologous protein has a destabilizing effect on nanoparticles auto-assembly efficacy. This destabilizing effect can be compensated by external or internal peptide insertion within the particles.
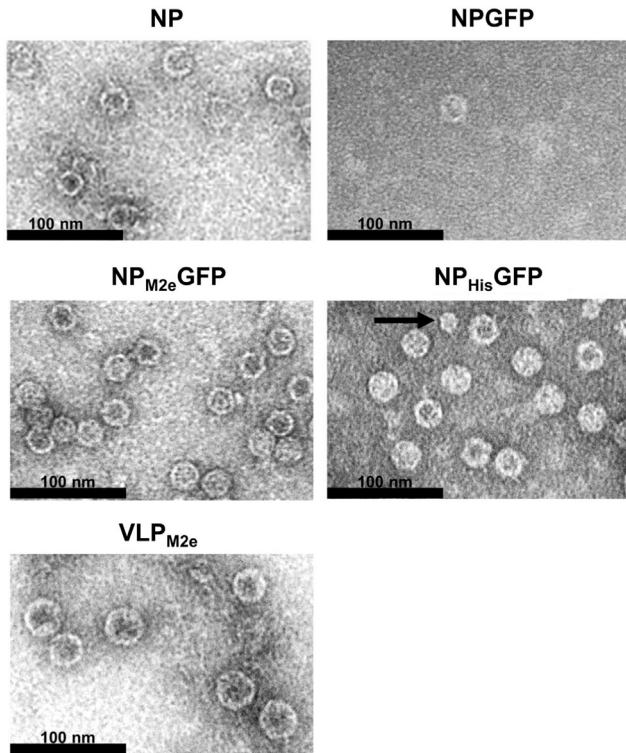
Fig. 4. Structural characterization of engineered nanoparticles by electronic microscopy.

3.3. Surface engineering of encapsulin nanoparticles enhances their cargo loading capacity

In order to evaluate the cargo loading capacity of generated nanoparticles, we estimated the molecular ratios of the component encapsulin and GFP proteins. GFP concentration was estimated by fluorescence and substracted to total protein concentration to estimate encapsulin concentration. Molar ratios between the two proteins were calculated considering the molecular weight of a 60 monomer encapsulin nanoparticle.

We evaluated the loading capacity from the ratio of the concentrations of encapsulin and GFP based on the fact that 60 monomers auto-assemble to form one nanoparticle. As shown in Table 1, and Fig. 4, no GFP or only one molecule per nanoparticle was associated to NPGFP and NP$_{His}$GFP nanoparticles respectively. In sharp contrast, an estimate of 30 GFP molecules was packaged in each NP$_{M2e}$GFP nanoparticle. These results suggest that the internal His-

tidine peptide may hide access to the hydrophobic internal binding pocket of the flp tag whereas the surface M2e epitope, in addition to its stabilizing effect on assembly, enhances the loading capacity of heterologous cargos into nanoparticles.

3.4. Engineered encapsulin nanoparticles elicit antibody responses against surface displayed epitope and engineered payload

In order to assess the immunogenicity of NP$_{M2E}$GFP encapsulin nanoparticles against the exposed flu epitope and the packaged heterologous protein, mice were immunized 3 times, at 2 weeks intervals with 50 μg of purified nanoparticles in presence of Freund's adjuvants. The antibody responses were measured individually at day 42. As shown in Fig. 5A, immunization with NP$_{M2e}$GFP induced antibodies that recognize the surface epitope M2e. These IgG titers were comparable to the titers obtained with VLP$_{M2e}$ used as reference. The capacity to induce antibodies against the packaged heterologous protein is shown in Fig. 5B. Therefore, antibody responses induced with NP$_{M2e}$GFP and GFP were compared. Immunization with NP$_{M2e}$GFP induced GFP specific antibodies. These IgG titers were about $2\log_{10}$ lower when compared to the group immunized with GFP.

4. Discussion

In the present study we describe the engineering of *T. maritima* encapsulin nanoparticles as a versatile platform for simultaneous presentation of epitopes at the nanoparticle surface as well as the packaging of heterologous proteins inside the particle. We show that encapsulin surface engineering has a positive effect on particle assembly stability and loading capacity. Immunogenicity assays in mice revealed that specific antibody titers could be induced against both engineered surface epitope M2e and heterologous cargo protein GFP, demonstrating the versatility of encapsulin nanoparticles for both surface display and vectorization.

Without considering surface engineering, our results obtained from wild type encapsulin engineering with and without heterologous protein loading (NPGFP versus NP) and with an additional internal HexaHistidine peptide (NP$_{His}$GFP) indicate (i) that cargo-free encapsulin (NP) from *T. maritima* expressed in *E coli* auto-assembles to form correctly shaped icosahedral nanoparticles; (ii) that loading of heterologous reporter protein to the encapsulin adding flp sequence responsible for cargo loading (construct NPGFP) results in the formation of very few correctly assembled nanoparticles and (iii) that the addition of six consecutive histidines at position 42 (construct NP$_{HIS}$GFP) leads to improved auto-assembly and stability of particles while loading efficacy remained very low. All these observations are in accordance with previous
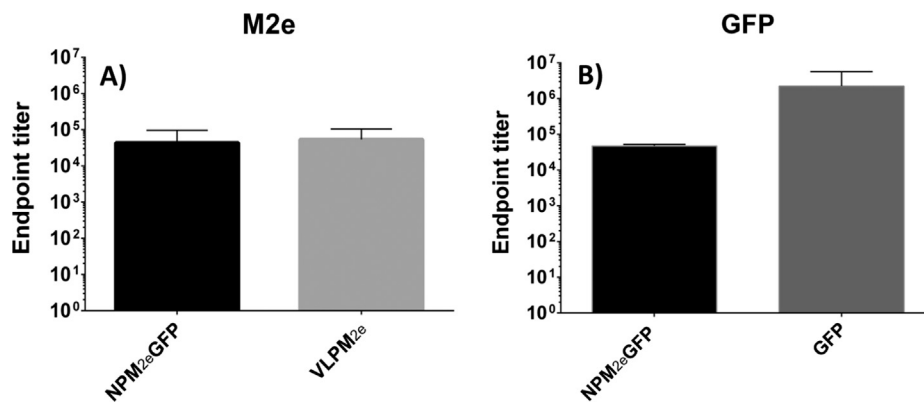

Fig. 5. Evaluation of humoral immune response. Antibody response against epitope M2e (A) and against GFP (B).

findings [24,33,34]. Snijder and collaborators [35] demonstrated, using a combination of mass spectrometry, atomic force microscopy and a multiscale molecular modeling approach, that protein loading has a destabilizing effect on nanoparticle assembly from *B. linens* and *T. maritima*. The authors suggest that localized binding of the cargo proteins within the shell may be responsible for local symmetry break. Alternatively, the mechanism of destabilizing effect might be similar to the one recently described for artificially loaded virus-derived cages [40]. Several studies have demonstrated that loading capacity varies from one heterologous reporter protein in encapsulin nanocompartment of *R. erythropolis* N771 to maximal 12 cargo protein in encapsulin nanoparticles from *B. linens* and *T maritima* [32,34]. These loading efficiency variations might be due to the type of protein loaded as well as to the type of encapsulin tested. Comparing NPGFP and NP$_{His}$GFP, the improved assembly using HexaHis peptide may be explained by the heat stabilizing effect up to 90 °C previously described [33]. However, loading capacity is not improved probably due to the fact that internal His sequence insertion hides access to the hydrophobic binding pocket, rich in proline, alanine and glycine serving as anchor sequence for the flp tag [24] and therefore prevents interaction supposedly by physical hindrance.

In contrast to the results obtained with encapsulin GFP cargo (NPGFP), engineering of the particle surface, and in particular the insertion of the ectodomain of matrix protein M2e from *Influenza A* virus H1N1 between amino acid positions 138 and 139 (NP$_{M2e}$-GFP), significantly improves the cargo protein loading capacity. A study on mechanistic properties [34] revealed that encapsulin is an elastic modulus of the shell. We hypothesize that the insertion of the M2e peptide induces a critical elastic deformation resulting in improved stiffness that could contribute to a greater cargo capacity of the particle. Our results strongly suggest that the M2e encapsulin surface engineering is responsible for the increased loading capacity. A cell penetrating peptide sequence for targeted delivery has been inserted at this position, however no effect on cargo loading has been assessed [33]. We are currently investigating the surface engineering of the particles for improved loading capacity. For this purpose we generated a construct with increased insertion capability up to 55 amino-acids (NP$_{55}$GFP, data not shown). Our preliminary results indicate that correctly assembled icosahedral nanoparticles are obtained and loading capacity remains unchanged. Future work on conjugation approaches for surface functionalization may enable entire vaccine antigen display [4,16,41]. These conjugation systems might allow increased flexibility (i) for the production process, producing the cargo loaded nanoparticles as low cost carriers directly in *E coli* whereas the antigens to be displayed can be expressed in a different expression system and (ii) for appropriate design of antigens or epitopes to increase immunogenicity [13,42].

Interestingly these first immunogenicity results on encapsulin nanoparticles show that simultaneous M2e surface display and GFP loading (construct NP$_{M2e}$GFP) can induce specific antibodies against both M2e surface epitope and the loaded GFP in our experimental conditions. Importantly M2e antibody response is similar with both types of nanoparticles tested (encapsulin and bacteriophage MS2), demonstrating the versatile potential of encapsulin nanoparticles in the field of vaccinology. Packaging of immunomodulating molecules like flagellin, pilin or lipoproteins could be of interest for rational vaccine design. We also tested whether specific antibodies are induced against the encapsulin carrier. Our preliminary results confirm antibody titer generation against the encapsulin nanoparticles. Previous findings of antibody levels raised against bacteriophage mediated VLP have been described [4,17]. Moreover, the promising malaria vaccine RTS,S consisting of a repeated sequences from *Plasmodium falciparum* circumsporozoite protein fused to the hepatitis B surface carrier has shown to induce an increase of anti-HBs antibodies after the first administration [43]. However, RTS,S vaccine passed the phase III evaluation and Qβ VLP conjugated with beta amyloid peptide is under phase III for the treatment of Alzheimer disease [44].

To conclude, we have shown that surface engineering of encapsulin nanoparticles has a positive effect on loading capacity of heterologous proteins. Furthermore, immunogenicity assays in mice have indicated specific antibody titers against both engineered surface epitope M2e and heterologous cargo protein GFP, demonstrating the aptitude of encapsulin nanoparticles for both surface display and vectorization. Taken together, these results suggest that encapsulin engineered nanoparticles with simultaneous surface display and packaging of antigens have potential for rational vaccine design and vectorization.

Funding

Conflict of interest

PL, AL and BW are inventors on a patent application that has been filed in relation with some aspects of this work.

Authors' contributions

BW and AL conceived and supervised the study; AL and PL designed experiments; PL, CM and SD performed experiments; CM provided new tools and reagents; JM did electronic microscopy analysis and interpretation, PL, CM, AL, SP and BW analyzed data; BW and PL wrote the manuscript; AL, PL, GS, CM, and BW made manuscript revisions, BW did final approval.

Acknowledgements

References

[1] Plotkin SA, Plotkin SL. The development of vaccines: how the past led to the future. Nat Rev Microbiol 2011;9(12):889–93.
[2] Patterson AR et al. Interlaboratory comparison of Porcine circovirus-2 indirect immunofluorescent antibody test and enzyme-linked immunosorbent assay results on experimentally infected pigs. J Vet Diagn Invest 2011;23(2):206–12.
[3] Gomes AC, Mohsen M, Bachmann MF. Harnessing nanoparticles for immunomodulation and vaccines. Vaccines (Basel) 2017;5(1).
[4] Gomes AC et al. Adjusted particle size eliminates the need of linkage of antigen and adjuvants for appropriated t cell responses in virus-like particle-based vaccines. Front Immunol 2017;8:226.
[5] Rampling T et al. Safety and high level efficacy of the combination malaria vaccine regimen of RTS, S/AS01B with chimpanzee adenovirus 63 and modified vaccinia ankara vectored vaccines expressing ME-TRAP. J Infect Dis 2016;214 (5):772–81.
[6] Giessen TW. Encapsulins: microbial nanocompartments with applications in biomedicine, nanobiotechnology and materials science. Curr Opin Chem Biol 2016;34:1–10.
[7] Maham A et al. Protein-based nanomedicine platforms for drug delivery. Small 2009;5(15):1706–21.
[8] Gabizon AA. Stealth liposomes and tumor targeting: one step further in the quest for the magic bullet. Clin Cancer Res 2001;7(2):223–5.
[9] Haag R, Kratz F. Polymer therapeutics: concepts and applications. Angew Chem Int Ed Engl 2006;45(8):1198–215.
[10] Liechty WB et al. Polymers for drug delivery systems. Annu Rev Chem Biomol Eng 2010;1:149–73.
[11] Sun C, Lee JS, Zhang M. Magnetic nanoparticles in MR imaging and drug delivery. Adv Drug Deliv Rev 2008;60(11):1252–65.
[12] Negahdaripour M et al. Harnessing self-assembled peptide nanoparticles in epitope vaccine design. Biotechnol Adv 2017;35(5):575–96.

[13] Bachmann MF, Jennings GT. Vaccine delivery: a matter of size, geometry, kinetics and molecular patterns. Nat Rev Immunol 2010;10(11):787–96.

[14] Rohovie MJ, Nagasawa M, Swartz JR. Virus-like particles: Next-generation nanoparticles for targeted therapeutic delivery. Bioeng Transl Med 2017;2(1):43–57.

[15] Pushko P, Pumpens P, Grens E. Development of virus-like particle technology from small highly symmetric to large complex virus-like particle structures. Intervirology 2013;56(3):141–65.

[16] Brune KD et al. Plug-and-Display: decoration of Virus-Like Particles via isopeptide bonds for modular immunization. Sci Rep 2016;6:19234.

[17] Tissot AC et al. Versatile virus-like particle carrier for epitope based vaccines. PLoS One 2010;5(3):e9809.

[18] Doucet M et al. Preclinical development of a vaccine against oligomeric alpha-synuclein based on virus-like particles. PLoS ONE 2017;12(8):e0181844.

[19] Pumpens P et al. The true story and advantages of RNA phage capsids as nanotools. Intervirology 2016;59(2):74–110.

[20] Ramirez A et al. A virus-like particle vaccine candidate for influenza A virus based on multiple conserved antigens presented on hepatitis B tandem core particles. Vaccine 2018.

[21] Kaba SA et al. Self-assembling protein nanoparticles with built-in flagellin domains increases protective efficacy of a Plasmodium falciparum based vaccine. Vaccine 2017.

[22] Zabel F, Kundig TM, Bachmann MF. Virus-induced humoral immunity: on how B cell responses are initiated. Curr Opin Virol 2013;3(3):357–62.

[23] Yan D et al. The application of virus-like particles as vaccines and biological vehicles. Appl Microbiol Biotechnol 2015;99(24):10415–32.

[24] Sutter M et al. Structural basis of enzyme encapsulation into a bacterial nanocompartment. Nat Struct Mol Biol 2008;15(9):939–47.

[25] Akita F et al. The crystal structure of a virus-like particle from the hyperthermophilic archaeon Pyrococcus furiosus provides insight into the evolution of viruses. J Mol Biol 2007;368(5):1469–83.

[26] Rosenkrands I et al. Identification and characterization of a 29-kilodalton protein from Mycobacterium tuberculosis culture filtrate recognized by mouse memory effector cells. Infect Immun 1998;66(6):2728–35.

[27] Valdes-Stauber N, Scherer S. Nucleotide sequence and taxonomical distribution of the bacteriocin gene lin cloned from Brevibacterium linens M18. Appl Environ Microbiol 1996;62(4):1283–6.

[28] McHugh CA et al. A virus capsid-like nanocompartment that stores iron and protects bacteria from oxidative stress. Embo j 2014;33(17):1896–911.

[29] Contreras H et al. Characterization of a Mycobacterium tuberculosis nanocompartment and its potential cargo proteins. J Biol Chem 2014;289(26):18279–89.

[30] Rahmanpour R, Bugg TD. Assembly in vitro of Rhodococcus jostii RHA1 encapsulin and peroxidase DypB to form a nanocompartment. Febs j 2013;280(9):2097–104.

[31] Rurup WF et al. Self-sorting of foreign proteins in a bacterial nanocompartment. J Am Chem Soc 2014;136(10):3828–32.

[32] Tamura A et al. Packaging guest proteins into the encapsulin nanocompartment from Rhodococcus erythropolis N771. Biotechnol Bioeng 2015;112(1):13–20.

[33] Moon H et al. Developing genetically engineered encapsulin protein cage nanoparticles as a targeted delivery nanoplatform. Biomacromolecules 2014;15(10):3794–801.

[34] Snijder J et al. Defining the stoichiometry and cargo load of viral and bacterial nanoparticles by orbitrap mass spectrometry. J Am Chem Soc 2014;136(20):7295–9.

[35] Snijder J et al. Assembly and mechanical properties of the cargo-free and cargo-loaded bacterial nanocompartment encapsulin. Biomacromolecules 2016;17(8):2522–9.

[36] Fiers W et al. A "universal" human influenza A vaccine. Virus Res 2004;103(1–2):173–6.

[37] Karimi M et al. Nanocaged platforms: modification, drug delivery and nanotoxicity. Opening synthetic cages to release the tiger. Nanoscale 2017;9(4):1356–92.

[38] Lagoutte P et al. Scalable chromatography-based purification of virus-like particle carrier for epitope based influenza A vaccine produced in Escherichia coli. J Virol Methods 2016;232:8–11.

[39] Mast J, Demeestere L. Electron tomography of negatively stained complex viruses: application in their diagnosis. Diagn Pathol 2009;4:5.

[40] Llauro A et al. Cargo-shell and cargo-cargo couplings govern the mechanics of artificially loaded virus-derived cages. Nanoscale 2016;8(17):9328–36.

[41] Thrane S et al. Bacterial superglue enables easy development of efficient virus-like particle based vaccines. J Nanobiotechnol 2016;14:30.

[42] Smith DM, Simon JK, Baker Jr JR. Applications of nanotechnology for immunology. Nat Rev Immunol 2013;13(8):592–605.

[43] Leroux-Roels G et al. Evaluation of the immune response to RTS, S/AS01 and RTS, S/AS02 adjuvanted vaccines: randomized, double-blind study in malaria-naive adults. Hum Vaccin Immunother 2014;10(8):2211–9.

[44] Vandenberghe R et al. Active Abeta immunotherapy CAD106 in Alzheimer's disease: A phase 2b study. Alzheimers Dement (N Y) 2017;3(1):10–22.